Bifurcation Structure of Equilibria of Adaptation Dynamics in Self-Organizing Neural Networks

Peter Tiňo
School of Computer Science
The University of Birmingham
Birmingham B15 2TT, UK

Abstract

Self-organizing neural networks (SONN) driven by softmax weight renormalization are capable of finding high quality solutions of difficult assignment optimization problems. Renormalization of assignment weights is shaped by a temperature parameter. As the system cools down the assignment weights become increasingly crisp. It has been reported that SONN search process can exhibit complex adaptation patterns as the system cools down. Moreover, there exists a critical temperature setting at which SONN is capable of powerful intermittent search through a multitude of high quality solutions represented as meta-stable states. In order to shed light on such observed phenomena, we present a detailed bifurcation study of the renormalization process and for each emerging equilibrium give exact characterization of stable/unstable manifolds of the linearized dynamics. As SONN cools down, new renormalization equilibria emerge in a strong structure until finally a complex skeleton of saddle type equilibria surrounding an unstable maximum entropy point, with decision enforcing "one-hot" stable equilibria emerges. This, in synergy with the SONN input driving process, can lead to sensitivity to annealing schedules and adaptation dynamics exhibiting signatures of complex dynamical behavior. We also rigorously show that (as hypothesized in earlier studies) the intermittent search by SONN can occur only at temperatures close to the first (symmetry breaking) bifurcation temperature.

1 Introduction

For more than two decades there has been an energetic research activity on application of neural computation techniques in solving difficult combinatorial optimization problems (Smith, 1999). Self-organizing neural network

(SONN) (Smith, 1995) constitutes an example of a successful neural-based methodology for solving 0-1 assignment problems. SONN has been successfully applied in a wide variety of applications, from assembly line sequencing to frequency assignment in mobile communications (Smith et al., 1998).

As in most self-organizing systems, dynamics of SONN adaptation is driven by a synergy of cooperation and competition. In the spirit of self-organizing feature maps (Kohonen, 1990), in the competition phase, the best candidate for the assignment among all possible candidates is selected and the corresponding assignment weight is increased. In the cooperation phase, the assignment weights of other candidates that were likely to be selected, but were not quite as strong as the selected one, get increased as well, albeit to a lesser degree.

For each item to be assigned the assignment weights need to be positive and sum to 1, i.e. they live on a standard simplex. Therefore, after each SONN adaptation phase, the assignment weights need to be renormalized back onto the standard simplex. Typically softmax function is employed (Guerrero et al., 2002). When endowed with a physics-based Boltzmann distribution interpretation, the softmax function contains a temperature parameter $T > 0$. As the system cools down, the assignments become increasingly crisp.

In the original setting SONN is annealed so that a single high quality solution to an assignment problem is found. However, interesting and quite surprising observations have been made recently regarding the temperature settings in the softmax renormalization step (Kwok and Smith, 2005). There exists a critical temperature T_* at which SONN is capable of powerful intermittent search through a multitude of high quality solutions represented as meta-stable states of the SONN dynamics. Kwok and Smith (2005) hypothesize that the critical temperature may be closely related to the symmetry breaking bifurcation of equilibria in the autonomous softmax dynamics. However, at present there is still no theory regarding the dynamics of SONN adaptation driven by the softmax renormalization. Consequently, the processes of crystallising a solution in an annealed version of SONN, or of sampling the solution space in the intermittent search regime are far from being understood.

The first steps towards theoretical underpinning of SONN adaptation driven by softmax renormalization were taken in (Kwok and Smith, 2004, 2005; Tiňo, 2007). For example, Kwok and Smith (2004) take the view of the whole SONN as a dynamical system and treats the temperature T as a bifurcation parameter. The cooperation phase was not included in the model. The renormalization process was empirically shown to result in

complicated bifurcation patterns revealing a complex nature of the search process inside SONN as the systems gets annealed. Indeed, renormalization onto the standard simplex is a double edged sword. On one hand, SONN with assignment weight renormalization have empirically shown sensitivity to annealing schedules, on the other hand, the quality of solutions could be greatly improved (Kwok and Smith, 2000).

Kwok and Smith (2005) suggested to study SONN adaptation dynamics by concentrating on the autonomous renormalization process, since it is this process that underpins the search dynamics in the SONN. In our previous paper (Tiňo, 2007) we initiated a rigorous study of equilibria of the autonomous renormalization process and found analytical approximations to the critical temperature as a function of SONN size. In this paper we complement (Tiňo, 2007) by performing a detailed bifurcation study of the renormalization process and give precise characterization and stability types of equilibria, as they emerge during the annealing process. Interesting and intricate equilibria structure emerges as the system cools down, explaining empirically observed complexity of SONN adaptation during intermediate stages of the annealing process. The analysis also clarifies why the intermittent search by SONN occurs near the first (symmetry breaking) bifurcation temperature of the renormalization step, as was experimentally verified in (Kwok and Smith, 2005; Tiňo, 2007).

The paper has the following organization: After a brief introduction to SONN and autonomous renormalization in sections 2 and 3, respectively, we study the emerging structure and stability types of renormalization equilibria in sections 4 and 5. The results are then discussed in section 6 and we summarize the key findings in section 7.

2 Self-Organizing Neural Network with softmax weight renormalization

Let us first briefly introduce Self-Organizing Neural Network (SONN) endowed with weight renormalization for solving assignment optimization problems (see e.g. (Kwok and Smith, 2005)). Consider a finite set of input elements (neurons) $i \in \mathcal{I} = \{1, 2, ..., M\}$ that need to be assigned to outputs (output neurons) $j \in \mathcal{J} = \{1, 2, ..., N\}$, so that some global cost of an assignment $\mathcal{A} : \mathcal{I} \to \mathcal{J}$ is minimized. Partial cost of assigning $i \in \mathcal{I}$ to $j \in \mathcal{J}$ is denoted by $V(i, j)$. The "strength" of assigning i to j is represented by the "assignment weight" $w_{i,j} \in (0, 1)$.

The SONN algorithm consists of:

1. Initializing connection weights $w_{i,j}$, $i \in \mathcal{I}$, $j \in \mathcal{J}$, to small random values.

2. Choosing at random an output item $j_c \in \mathcal{J}$ and calculating partial costs $V(i, j_c)$ incurred by assigning all possible input elements $i \in \mathcal{I}$ to j_c.

3. Selecting the winner input element (neuron) $i(j_c) \in \mathcal{I}$ that minimizes $V(i, j_c)$. Often the winner-takes-all approach is softened by considering other reasonable, albeit not as strong candidates: the "neighborhood" $\mathcal{B}_L(i(j_c))$ of size L of the winner node $i(j_c)$ consists of L nodes $i \neq i(j_c)$ that yield the smallest partial costs $V(i, j_c)$.

4. Weights from nodes $i \in \mathcal{B}_L(i(j_c))$ to j_c get strengthened:

$$w_{i,j_c} \leftarrow w_{i,j_c} + \eta(i)(1 - w_{i,j_c}), \quad i \in \mathcal{B}_L(i(j_c)),$$

   where $\eta(i)$ is proportional to the quality of assignment $i \rightarrow j_c$, as measured by $V(i, j_c)$.

5. Weights[1] $\mathbf{w}_i = (w_{i,1}, w_{i,2}, ..., w_{i,N})'$ for each input node $i \in \mathcal{I}$ are normalized using softmax

$$w_{i,j} \leftarrow \frac{\exp(\frac{w_{i,j}}{T})}{\sum_{k=1}^{N} \exp(\frac{w_{i,k}}{T})}.$$

6. Repeat from step 2 until all output nodes $j_c \in \mathcal{J}$ have been selected (one epoch).

Even though the soft assignments $w_{i,j}$ evolve in continuous space, when needed, a 0-1 assignment solution can be produced by imposing $\mathcal{A}(i) = j$ if and only if $j = \text{argmax}_{k \in \mathcal{I}} w_{i,k}$.

We will refer to SONN for solving an (M, N)-assignment problem as (M, N)-SONN. As mentioned earlier, following (Kwok and Smith, 2005; Tiňo, 2007) we strive to understand the search dynamics inside SONN by analyzing the autonomous dynamics of the renormalization update step 5 of the SONN algorithm.

[1] here $'$ denotes the transpose operator

3 Iterative softmax

The weight vector $\mathbf{w}_i$ of each of M neurons in an (M, N)-SONN lives in the *standard* $(N-1)$-*simplex*,

$$S_{N-1} = \{\mathbf{w} = (w_1, w_2, ..., w_N)' \in \mathbb{R}^N \mid w_i \geq 0, i = 1, 2, ..., N, \text{ and } \sum_{i=1}^{N} w_i = 1\}. \tag{1}$$

Given a value of the temperature parameter $T > 0$, the softmax renormalization step in SONN adaptation transforms the weight vector of each unit as follows:

$$\mathbf{w} \mapsto \mathbf{F}(\mathbf{w}; T) = (F_1(\mathbf{w}; T), F_2(\mathbf{w}; T), ..., F_N(\mathbf{w}; T))', \tag{2}$$

where

$$F_i(\mathbf{w}; T) = \frac{\exp(\frac{w_i}{T})}{Z(\mathbf{w}; T)}, \quad i = 1, 2, ..., N, \tag{3}$$

and

$$Z(\mathbf{w}; T) = \sum_{k=1}^{N} \exp(\frac{w_k}{T}) \tag{4}$$

is the normalization factor. Formally, $\mathbf{F}$ maps $\mathbb{R}^N$ to S^0_{N-1}, the interior of S_{N-1}:

$$S^0_{N-1} = \{\mathbf{w} \in \mathbb{R}^N \mid w_i > 0, i = 1, 2, ..., N, \text{ and } \sum_{i=1}^{N} w_i = 1\}. \tag{5}$$

Linearization of $\mathbf{F}$ around $\mathbf{w} \in S^0_{N-1}$ is given by the (symmetric) Jacobian $J(\mathbf{w}; T)$:

$$J(\mathbf{w}; T)_{i,j} = \frac{1}{T}[\delta_{i,j} F_i(\mathbf{w}; T) - F_i(\mathbf{w}; T) F_j(\mathbf{w}; T)], \quad i, j = 1, 2, ..., N, \tag{6}$$

where $\delta_{i,j} = 1$ iff $i = j$ and $\delta_{i,j} = 0$ otherwise.

The softmax map $\mathbf{F}$ induces on S^0_{N-1} a discrete time dynamics known as *Iterative Softmax* (ISM):

$$\mathbf{w}(t+1) = \mathbf{F}(\mathbf{w}(t); T). \tag{7}$$

The renormalization step in an (M, N)-SONN adaptation involves M separate renormalizations of weight vectors of all of the M SONN units.

Denoting by $\mathbf{w}_i$, $i = 1, 2, ..., M$, the weight vector of i-th unit, the SONN renormalization step,

$$\mathbf{W} = (\mathbf{w}_1', \mathbf{w}_2', ..., \mathbf{w}_M')' \mapsto \mathcal{F}(\mathbf{W}; T) = (\mathbf{F}(\mathbf{w}_1; T)', \mathbf{F}(\mathbf{w}_2; T)', ..., \mathbf{F}(\mathbf{w}_M; T)')', \tag{8}$$

takes $(S_{N-1}^0)^M$ to itself. In the renormalization step, the softmax map $\mathbf{F}$ operates on M simplexes separately, but note that the weights of different units are coupled by the Hebbian SONN adaptation step 4 in section 2. The renormalization map $\mathcal{F}$ induces on $(S_{N-1}^0)^M$ dynamics

$$\mathbf{W}(t+1) = \mathcal{F}(\mathbf{W}(t); T). \tag{9}$$

It has been argued (Kwok and Smith, 2003, 2004, 2005; Tiňo, 2007) that a detailed knowledge of the *autonomous* renormalization step dynamics in SONN training is crucial for understanding the process of searching for solutions by SONN, both in the intermittent search regime (Kwok and Smith, 2003, 2005; Tiňo, 2007), and in the original annealed regime (Kwok and Smith, 2004). The normalization process has not been studied theoretically in a detailed manner, although (Kwok and Smith, 2005; Tiňo, 2007) offer first steps in that direction.

In the next section we study in detail the mechanism of emergence of a complicated structure of equilibria of the SONN renormalization step, as the system gets annealed. We will study systems for $N \geq 2$.

4 Equilibria of SONN renormalization step

Note that the renormalization dynamics (9), viewed as an autonomous dynamical system, can be decomposed into M decoupled dynamics,

$$\mathbf{w}_i(t+1) = \mathbf{F}(\mathbf{w}_i(t); T), \quad i = 1, 2, ..., M, \tag{10}$$

each operating on the interior S_{N-1}^0 of the standard $(N-1)$-simplex. It follows that for each temperature setting T, the structure of equilibria in the i-th system, $\mathbf{w}_i(t+1) = \mathbf{F}(\mathbf{w}_i(t); T)$, gets copied in all the other $M-1$ systems. Using this symmetry, it is sufficient to concentrate on a single ISM (7).

4.1 Notation and background material

First, we introduce basic concepts and notation that will be used throughout the paper.

In general, an $(n-1)$-*simplex* is just the convex hull of a set of n affinely independent points in $\mathbb{R}^m$, $m \geq n-1$. A special case is the standard $(N-1)$-simplex S_{N-1} defined in (1). It is the convex hull of the standard basis of $\mathbb{R}^N$, $\{\mathbf{e}_1, \mathbf{e}_2, ..., \mathbf{e}_N\}$, where $\mathbf{e}_i$ is an N-dimensional vector of 0's, except for the coordinate i that has value 1.

The convex hull of any nonempty subset of n vertices of an $(r-1)$-simplex Δ, $n \leq r$, is called an $(n-1)$-*face* of Δ. There are $\binom{r}{n}$ distinct $(n-1)$-faces of Δ. Each $(n-1)$-face is an $(n-1)$-simplex. In particular, the 0-faces and 1-faces are the vertices and edges, respectively, of Δ. The $(r-2)$-faces are the facets of Δ. Obviously, the unique $(r-1)$-face of Δ is the simplex Δ itself.

Given a set of n vertices $\mathbf{w}_1, \mathbf{w}_2, ..., \mathbf{w}_n \in \mathbb{R}^m$ defining an $(n-1)$-simplex Δ in $\mathbb{R}^m$, the central point,

$$\overline{\mathbf{w}}(\Delta) = \frac{1}{n} \sum_{i=1}^{n} \mathbf{w}_i, \tag{11}$$

is called the maximum entropy point of Δ.

We will denote the set of all $(n-1)$-faces of the standard $(N-1)$-simplex S_{N-1} by $\mathcal{P}_{N,n}$. The set of their maximum entropy points is denoted by $\mathcal{Q}_{N,n}$, i.e.

$$\mathcal{Q}_{N,n} = \{\overline{\mathbf{w}}(\Delta) |\ \Delta \in \mathcal{P}_{N,n}\}. \tag{12}$$

The n-dimensional column vectors of 1's and 0's are denoted by $\mathbf{1}_n$ and $\mathbf{0}_n$, respectively. Note that

$$\overline{\mathbf{w}}_{N,n} = \frac{1}{n}(\mathbf{1}_n', \mathbf{0}_{N-n}')' \tag{13}$$

is in $\mathcal{Q}_{N,n}$. In addition, all the other elements of $\mathcal{Q}_{N,n}$ can be obtained by simply permuting coordinates of $\overline{\mathbf{w}}_{N,n}$. Due to this symmetry, we will be able to develop most of the material using $\overline{\mathbf{w}}_{N,n}$ only and then transfer the results to permutations of $\overline{\mathbf{w}}_{N,n}$. The maximum entropy point $\overline{\mathbf{w}}_{N,N} = N^{-1}\mathbf{1}_N$ of the standard $(N-1)$-simplex S_{N-1} will often be denoted simply by $\overline{\mathbf{w}}$. To simplify the notation we will use $\overline{\mathbf{w}}$ to denote both the maximum entropy point of S_{N-1} and the vector $\overline{\mathbf{w}} - \mathbf{0}_N$.

Let us now briefly recall findings[2] of (Tiňo, 2007) that will be needed in this paper.

[2]presented here with a different notation, more suited for the presentation of this paper

The maximum entropy point $\overline{\mathbf{w}}$ is a fixed point of ISM (7) for any temperature setting T. All the other fixed points $\mathbf{w} = (w_1, w_2, ..., w_N)'$ of ISM have exactly two different coordinate values: $w_i \in \{\gamma_1, \gamma_2\}$, such that $N^{-1} < \gamma_1 < N_1^{-1}$ and $0 < \gamma_2 < N^{-1}$, where N_1 is the number of coordinates γ_1 larger than N^{-1}. Since $\mathbf{w} \in S_{N-1}^0$, we have

$$\gamma_2 = \frac{1 - N_1\gamma_1}{N - N_1}. \tag{14}$$

The number of coordinates γ_2 smaller than N^{-1} is denoted by N_2. Obviously, $N_2 = N - N_1$.

If $\mathbf{w} = (\gamma_1 \mathbf{1}'_{N_1}, \gamma_2 \mathbf{1}'_{N_2})'$ is a fixed point of ISM (7), so are all $\binom{N}{N_1}$ *distinct* permutations of it. We collect $\mathbf{w}$ and its permutations in a set defined as follows: given integers $N \geq 2$, $0 < N_1 < N$, and a real number $N^{-1} < \gamma_1 < N_1^{-1}$, we write

$$\mathcal{E}_{N,N_1}(\gamma_1) = \left\{ \mathbf{v} \in S_{N-1}^0 |\ \mathbf{v} \text{ is a permutation of } \left(\gamma_1 \mathbf{1}'_{N_1}, \frac{1 - N_1\gamma_1}{N - N_1} \mathbf{1}'_{N-N_1} \right)' \right\}. \tag{15}$$

The fixed points in $\mathcal{E}_{N,N_1}(\gamma_1)$ exist if and only if the temperature parameter T is set to

$$T_{N,N_1}(\gamma_1) = (N\gamma_1 - 1) \left[-(N - N_1) \cdot \ln \left(1 - \frac{N\gamma_1 - 1}{(N - N_1)\gamma_1} \right) \right]^{-1}. \tag{16}$$

For a given $N \geq 2$ and $0 < N_1 < N$, the temperature function $T_{N,N_1}(\gamma_1) : (N^{-1}, N_1^{-1}) \to \mathbb{R}^+$ is concave and

$$\lim_{\gamma_1 \to N^{-1}} T_{N,N_1}(\gamma_1) = N^{-1}. \tag{17}$$

In addition, the slope of $T_{N,N_1}(\gamma_1)$ at N^{-1} approaches

$$\kappa_{N,N_1} = \lim_{\gamma_1 \to N^{-1}} \frac{\mathrm{d}T_{N,N_1}(\gamma_1)}{\mathrm{d}\gamma_1} = 1 - \frac{N}{2(N - N_1)}. \tag{18}$$

For temperatures $T > 1/2$, the maximum entropy point $\overline{\mathbf{w}}$ is the unique equilibrium of ISM.

4.2 Bifurcations of equilibria of SONN renormalization

In this section we examine the mechanism of emergence of new equilibria of the SONN renormalization step, as the system anneals. As mentioned

earlier, the maximum entropy point $\overline{\mathbf{w}} = N^{-1}\mathbf{1}_N$ is a fixed point of ISM (7) for any temperature setting. The existence of other fixed points depends on the temperature T, as described by (16). We will show that as the system cools down, increasing number of equilibria emerge in a strong structure.

Let $\mathbf{w}, \mathbf{v} \in S_{N-1}$ be two points on the standard simplex. The line from $\mathbf{w}$ to $\mathbf{v}$ is parametrized as

$$\ell(\tau; \mathbf{w}, \mathbf{v}) = \mathbf{w} + \tau \cdot (\mathbf{v} - \mathbf{w}), \quad \tau \in [0, 1]. \tag{19}$$

Theorem 4.1 *All equilibria of ISM (7) lie on lines connecting the maximum entropy point $\overline{\mathbf{w}}$ of S_{N-1} with the maximum entropy points of its faces. In particular, for $0 < N_1 < N$ and $N^{-1} < \gamma_1 < N_1^{-1}$, all fixed points from $\mathcal{E}_{N,N_1}(\gamma_1)$ lie on lines $\ell(\tau; \overline{\mathbf{w}}, \mathbf{w})$, where $\mathbf{w} \in \mathcal{Q}_{N,N_1}$.*

Proof: We know that for a given $0 < N_1 < N$ and $N^{-1} < \gamma_1 < N_1^{-1}$, there is a temperature setting $T_{N,N_1}(\gamma_1)$ such that all permutations of $(\gamma_1 \mathbf{1}'_{N_1}, \gamma_2 \mathbf{1}'_{N_2})'$, where $N_2 = N - N_1$ and γ_2 is given by (14), are fixed points of ISM. Instead of dealing with the whole set $\mathcal{E}_{N,N_1}(\gamma_1)$, we will concentrate only on the representative $\mathbf{w}(\gamma_1) = (\gamma_1 \mathbf{1}'_{N_1}, \gamma_2 \mathbf{1}'_{N_2})'$; the result then follows by symmetry.

Consider the maximum entropy point $\overline{\mathbf{w}}_{N,N_1}$ of an $(N_1 - 1)$-face of S_{N-1} (see eq. (13)), $\overline{\mathbf{w}}_{N,N_1} = \frac{1}{N_1}(\mathbf{1}'_{N_1}, \mathbf{0}'_{N_2})'$. Then $\mathbf{w}(\gamma_1)$ lies on the line $\ell(\tau; \overline{\mathbf{w}}, \overline{\mathbf{w}}_{N,N_1})$ for the parameter setting $\tau = 1 - N\gamma_2$. In other words,

$$\gamma_1 = \frac{1}{N}\left(1 + \tau \frac{N_2}{N1}\right) \tag{20}$$

$$\gamma_2 = \frac{1}{N}(1 - \tau), \tag{21}$$

which can be easily verified by plugging in $\tau = 1 - N\gamma_2$ into (20). *Q.E.D.*

For an ISM fixed point $\mathbf{w} \in \mathcal{E}_{N,N_1}(\gamma_1)$ we will denote by $\Gamma(\mathbf{w})$ the maximum entropy point $\Gamma(\mathbf{w}) \in \mathcal{Q}_{N,N_1}$ of the $(N_1 - 1)$-face of S_{N-1}, such that $\mathbf{w} \in \ell(\tau; \overline{\mathbf{w}}, \Gamma(\mathbf{w}))$.

The result is illustrated in figure 1. Fixed points of ISM operating on the standard 3-simplex S_3 can only be found on the lines connecting the maximum entropy point $\overline{\mathbf{w}}$ (filled circle) with maximum entropy points of its faces. Triangles, squares and diamonds represent maximum entropy points of 0-faces (vertices), 1-faces (edges) and 2-faces (facets), respectively. Fixed

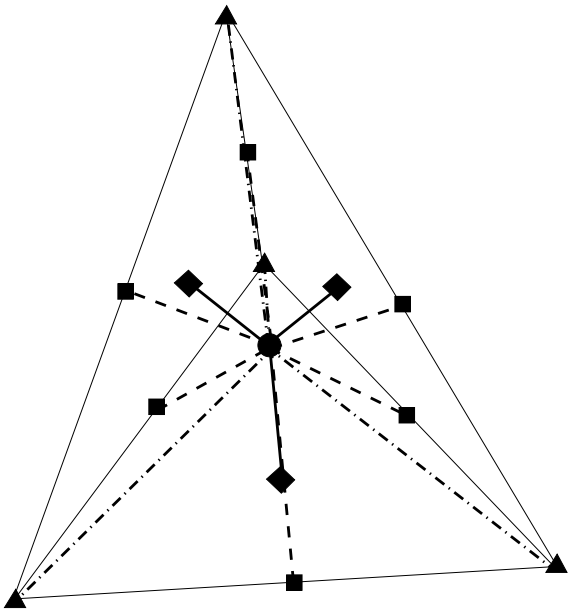

Figure 1: Positions of equilibria of SONN renormalization illustrated for the case of 4-dimensional weight vectors $\mathbf{w}$. ISM is operating on the standard 3-simplex S_3 and its equilibria can only be found on the lines connecting the maximum entropy point $\overline{\mathbf{w}}$ (filled circle) with maximum entropy points of its faces. Triangles, squares and diamonds represent maximum entropy points of 0-faces (vertices), 1-faces (edges) and 2-faces (facets), respectively.

points with three coordinates larger than 1/4 can be be found on the lines connecting $\overline{\mathbf{w}}$ with maximum entropy points of 2-faces (solid bold lines). Analogously, fixed points with two and one coordinate larger than 1/4 can be be found on the lines connecting $\overline{\mathbf{w}}$ with maximum entropy points of 1- and 0-faces (dashed and dashed-dotted bold lines, respectively).

Theorem 4.2 *For $N_1 < N/2$, there exists a temperature $T_E(N, N_1) > N^{-1}$ such that for $T \in (0, T_E(N, N_1)]$, ISM fixed points in $\mathcal{E}_{N,N_1}(\gamma_1)$ exist for some $\gamma_1 \in (N^{-1}, N_1^{-1})$, and no ISM fixed points in $\mathcal{E}_{N,N_1}(\gamma_1)$, for any $\gamma_1 \in (N^{-1}, N_1^{-1})$, can exist at temperatures $T > T_E(N, N_1)$. The temperature $T_E(N, N_1)$ is given by $T_{N,N_1}(\gamma_1^*)$, where γ_1^* is the unique solution of*

$$\ln\left[\frac{(N-N_1)\gamma_1}{1-N_1\gamma_1}\right] = \frac{\gamma_1 - \frac{1}{N}}{\gamma_1(1-N_1\gamma_1)}. \tag{22}$$

For each temperature $T \in (N^{-1}, T_E(N, N_1))$, there are two coordinate values $\gamma_1^-(T)$ and $\gamma_1^+(T)$, $N^{-1} < \gamma_1^-(T) < \gamma_1^+(T) < N_1^{-1}$, such that ISM fixed points in both $\mathcal{E}_{N,N_1}(\gamma_1^-(T))$ and $\mathcal{E}_{N,N_1}(\gamma_1^+(T))$ exist at temperature T. Furthermore, as the temperature decreases, $\gamma_1^-(T)$ decreases towards N^{-1}, while $\gamma_1^+(T)$ increases towards N_1^{-1}.

Proof: The temperature function $T_{N,N_1}(\gamma_1)$ (16) is concave and can be continuously extended to $[N^{-1}, N_1^{-1})$. At $\gamma_1 = N^{-1}$, the temperature is N^{-1} and since $N_1 < N/2$, the slope of $T_{N,N_1}(\gamma_1)$ at $\gamma_1 = N^{-1}$ is positive. Because

$$\lim_{\gamma_1 \to N_1^{-1}} T_{N,N_1}(\gamma_1) = 0 < N^{-1},$$

$T_{N,N_1}(\gamma_1)$ must have a unique maximum at some $\gamma_1^* \in (N^{-1}, N_1^{-1})$,

$$\gamma_1^* = \operatorname*{argmax}_{\gamma_1 \in (N^{-1}, N_1^{-1})} T_{N,N_1}(\gamma_1).$$

Setting the derivative of $T_{N,N_1}(\gamma_1)$ to zero leads to (22).

Obviously, no ISM fixed points in $\mathcal{E}_{N,N_1}(\gamma_1)$, for any $N^{-1} < \gamma_1 < N_1^{-1}$, can exist for temperatures greater than $T_{N,N_1}(\gamma_1^*)$.

Since $T_{N,N_1}(\gamma_1)$ is concave, for temperatures $N^{-1} < T < T_{N,N_1}(\gamma_1^*)$, there are two coordinate values $\gamma_1^-(T)$ and $\gamma_1^+(T)$, $\gamma_1^-(T) < \gamma_1^+(T)$, such that $T = T_{N,N_1}(\gamma_1^-(T)) = T_{N,N_1}(\gamma_1^+(T))$. The values $\gamma_1^-(T)$ and $\gamma_1 + (T)$ correspond to the increasing and decreasing branches of $T_{N,N_1}(\gamma_1)$, and so as the temperature decreases, $\gamma_1^-(T)$ decreases as well, while $\gamma_1^+(T)$ increases. *Q.E.D.*

Note that for low-temperature regimes, $T < N^{-1}$, there is only one value of $\gamma_1(T)$ close to N_1^{-1}, such that $T = T_{N,N_1}(\gamma_1(T))$. In other words, if $N_1 < N/2$, in low temperature regimes the fixed points tend to accumulate around the maximum entropy points of $(N_1 - 1)$-faces of S_{N-1}. The same is true for the ISM fixed points with $N_1 \geq N/2$ coordinates γ_1 larger than N^{-1}.

Theorem 4.3 *If $N/2 \leq N_1 < N$, for each temperature $T \in (0, N^{-1})$, there is exactly one coordinate value $\gamma_1(T) \in (N^{-1}, N_1^{-1})$, such that ISM fixed points in $\mathcal{E}_{N,N_1}(\gamma_1(T))$ exist at temperature T. No ISM fixed points in $\mathcal{E}_{N,N_1}(\gamma_1)$, for any $\gamma_1 \in (N^{-1}, N_1^{-1})$ can exist for temperatures $T > N^{-1}$. As the temperature decreases, $\gamma_1(T)$ increases towards N_1^{-1}.*

Proof: Since $N/2 \leq N_1 < N$, the slope of $T_{N,N_1}(\gamma_1)$ at $\gamma_1 = N^{-1}$ is not positive. In addition, $T_{N,N_1}(\gamma_1)$ is concave. It follows that for temperatures $T > N^{-1}$, there is no $\gamma_1(T)$ such that $T = T_{N,N_1}(\gamma_1(T))$. For $0 < T < N^{-1}$, $T_{N,N_1}(\gamma_1)$ is decreasing and there is exactly one $\gamma_1(T)$ such that $T = T_{N,N_1}(\gamma_1(T))$. *Q.E.D.*

Next, we will show that the set of bifurcation temperatures $T_E(N, N_1) > N^{-1}$, for $N_1 < N/2$, is linearly ordered.

Lemma 4.4 *Consider* $0 < N_1 < N_1' < N$ *and a coordinate value* $\gamma_1 \in (1/N, 1/N_1')$. *Then,*

$$\gamma_2 = \frac{1 - N_1\gamma_1}{N - N_1} > \frac{1 - N_1'\gamma_1}{N - N_1'} = \gamma_2'. \tag{23}$$

In addition, $T_{N,N_1'}(\gamma_1) < T_{N,N_1}(\gamma_1)$.

Proof: Let $N_1' = N_1 + 1$ and assume

$$\gamma_2 = \frac{1 - N_1\gamma_1}{N - N_1} \leq \frac{1 - (N_1 + 1)\gamma_1}{N - N_1 - 1} = \gamma_2'.$$

Then,

$$(N - N_1)(1 - N_1\gamma_1 - \gamma_1) \geq (N - N_1 - 1)(1 - N_1\gamma_1),$$

which is equivalent to $\gamma_1 \leq N^{-1}$. This is a contradiction. Hence, $\gamma_2 > \gamma_2'$. If $N_1' = N_1 + k$, for some $k > 1$, (23) can be obtained by induction.

Note that the temperature function can be re-written as

$$T_{N,N_1}(\gamma_1) = \frac{\gamma_1 - \gamma_2}{\ln\gamma_1 - \ln\gamma_2}, \tag{24}$$

with γ_2 given by (14).

Logarithm is a concave function. Since $0 < \gamma_2' < \gamma_2 < \gamma_1 < 1$, we have

$$T_{N,N_1}(\gamma_1) = \frac{\gamma_1 - \gamma_2}{\ln\gamma_1 - \ln\gamma_2} > \frac{\gamma_1 - \gamma_2'}{\ln\gamma_1 - \ln\gamma_2'} = T_{N,N_1'}(\gamma_1).$$

Q.E.D.

Theorem 4.5 *The bifurcation temperature* $T_E(N, N_1)$ *is decreasing with increasing number* N_1 *of equilibrium coordinates larger than* N^{-1}.

Proof: By lemma 4.4, for any feasible value of the larger coordinate $\gamma_1 > N^{-1}$, if there are two fixed points $\mathbf{w} \in \mathcal{E}_{N,N_1}(\gamma_1)$ and $\mathbf{w}' \in \mathcal{E}_{N,N_1'}(\gamma_1)$ of ISM, such that $N_1 < N_1'$, then $\mathbf{w}$ exists at a higher temperature than $\mathbf{w}'$ does.

For a given $N_1 < N/2$, the bifurcation temperature $T_E(N, N_1)$ corresponds to the maximum of $T_{N,N_1}(\gamma_1)$ on $\gamma_1 \in (N^{-1}, N_1^{-1})$. It follows that $N_1 < N_1'$ implies $T_E(N, N_1) > T_E(N, N_1')$. *Q.E.D.*

We now summarize the results of this section. For temperatures $T > 1/2$, the ISM has exactly one equilibrium - the maximum entropy point $\overline{\mathbf{w}}$ of S_{N-1}. As the temperature is lowered and hits the first bifurcation point, $T_E(N, 1)$, new fixed points of ISM emerge on the lines $\ell(\tau; \overline{\mathbf{w}}, \widetilde{\mathbf{w}})$, $\widetilde{\mathbf{w}} \in \mathcal{Q}_{N,1}$, one on each line. The lines connect $\overline{\mathbf{w}}$ with the vertices $\widetilde{\mathbf{w}}$ of S_{N-1}. As the temperature decreases further, on each line, the single fixed point splits into two fixed points, one moves towards $\overline{\mathbf{w}}$, the other moves towards the corresponding high entropy point $\widetilde{\mathbf{w}}$ in $\mathcal{Q}_{N,1}$ (vertex of S_{N-1}). When the temperature reaches the second bifurcation point, $T_E(N, 2)$, new fixed points of ISM emerge on the lines $\ell(\tau; \overline{\mathbf{w}}, \widetilde{\mathbf{w}})$, $\widetilde{\mathbf{w}} \in \mathcal{Q}_{N,2}$, one on each line. This time the lines connect $\overline{\mathbf{w}}$ with the maximum entropy points (midpoints) $\widetilde{\mathbf{w}}$ of the edges of S_{N-1}. Again, as the temperature continues decreasing, on each line, the single fixed point splits into two fixed points, one moves towards $\overline{\mathbf{w}}$, the other moves towards the corresponding maximum entropy point $\widetilde{\mathbf{w}}$ in $\mathcal{Q}_{N,2}$ (midpoint of an edge of S_{N-1}). Decreasing temperature further to $T_E(N, 3)$, new fixed points of ISM emerge on the lines $\ell(\tau; \overline{\mathbf{w}}, \widetilde{\mathbf{w}})$, $\widetilde{\mathbf{w}} \in \mathcal{Q}_{N,3}$, connecting $\overline{\mathbf{w}}$ with maximum entropy points $\widetilde{\mathbf{w}}$ of 2-faces of S_{N-1}. Decreasing the temperature even further, on each line, the single fixed point splits into two fixed points, one moves towards $\overline{\mathbf{w}}$, the other moves towards the corresponding maximum entropy point $\widetilde{\mathbf{w}}$ in $\mathcal{Q}_{N,3}$. The process continues until the last bifurcation temperature $T_E(N, N_1)$ is reached, where N_1 is the largest natural number smaller than $N/2$. At $T_E(N, N_1)$, new fixed points of ISM emerge on the lines $\ell(\tau; \overline{\mathbf{w}}, \widetilde{\mathbf{w}})$, $\widetilde{\mathbf{w}} \in \mathcal{Q}_{N,N_1}$, connecting $\overline{\mathbf{w}}$ with maximum entropy points $\widetilde{\mathbf{w}}$ of $(N_1 - 1)$-faces of S_{N-1}. As the temperature continues decreasing, on each line, the single fixed point splits into two fixed points, one moves towards $\overline{\mathbf{w}}$, the other moves towards the corresponding maximum entropy point $\widetilde{\mathbf{w}}$ in $\mathcal{Q}_{N,N_1}$. At temperatures below N^{-1}, only the fixed points moving towards the maximum entropy points of faces of S_{N-1} exist.

In the low temperature regime, $0 < T < N^{-1}$, a fixed point occurs on every line $\ell(\tau; \overline{\mathbf{w}}, \widetilde{\mathbf{w}})$, $\widetilde{\mathbf{w}} \in \mathcal{Q}_{N,N_1}$, $N_1 = \lceil N/2 \rceil, \lceil N/2 \rceil + 1, ..., N - 1$. Here, $\lceil x \rceil$ denotes the smallest integer y, such that $y \geq x$. As the temperature

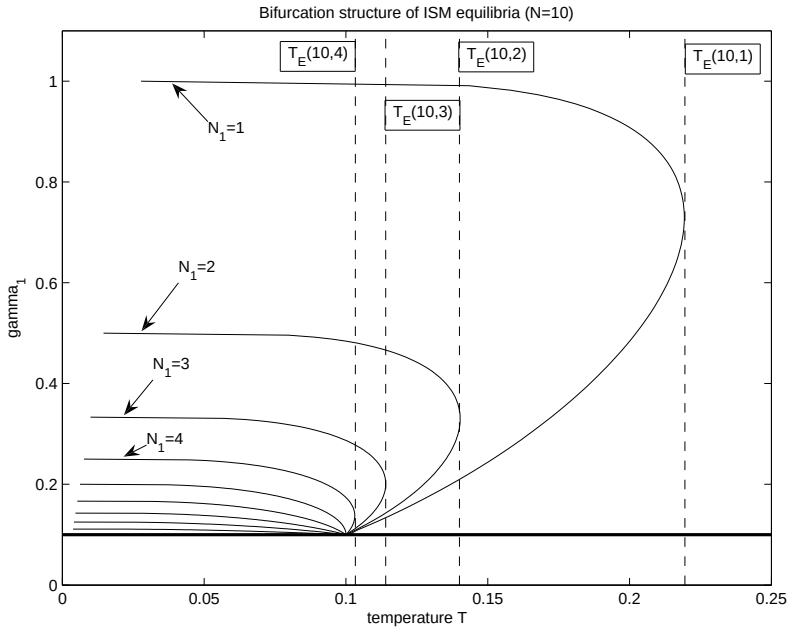

Figure 2: Demonstration of the process of creation of new ISM fixed points and their flow as the system temperature cools down. Here $N = 10$, e.g. the ISM operates on the standard 9-simplex S_9. Against each temperature setting T, the values of the larger coordinate $\gamma_1 > N^{-1}$ of the fixed points existing at T are plotted. The horizontal bold line corresponds to the maximum entropy point $\overline{\mathbf{w}} = 10^{-1}\mathbf{1}'_{10}$.

decreases, the fixed points $\mathbf{w}$ move towards the corresponding maximum entropy points $\Gamma(\mathbf{w}) = \widetilde{\mathbf{w}} \in \mathcal{Q}_{N,N_1}$ of $(N_1 - 1)$-faces of S_{N-1}.

The process of creation of new fixed points and their flow as the temperature cools down is demonstrated in figure 2 for an ISM operating on 9-simplex S_9. We plot against each temperature setting T the values of the larger coordinate $\gamma_1 > N^{-1} = 0.1$ of the fixed points existing at T.

Next theorem summarizes the number of fixed points of the SONN renormalization step, as a function of temperature T.

Theorem 4.6 *Consider an (M, N)-SONN for solving an (M, N) assignment problem. Then, at temperature $T > 0$, there exist $1 + \mathcal{N}_N(T)$ fixed points of ISM (7) and $(1 + \mathcal{N}_N(T))^M$ fixed points of the SONN renormal-*

ization step (9), where

1. *for temperatures* $T > T_E(N,1)$, $\mathcal{N}_N(T) = 0$,
2. *for temperatures* $T = T_E(N,N_1)$, $N_1 = 1,2,...,\lceil N/2\rceil - 1$,
$$\mathcal{N}_N(T) = \binom{N}{N_1} + 2\sum_{n=1}^{N_1-1}\binom{N}{n},$$
3. *for temperatures* $T_E(N,N_1) < T < T_E(N,N_1-1)$, $N_1 = 2,...,\lceil N/2\rceil - 1$,
$$\mathcal{N}_N(T) = 2\sum_{n=1}^{N_1-1}\binom{N}{n},$$
4. *for temperatures* $N^{-1} < T < T_E(N,\lceil N/2\rceil - 1)$,
$$\mathcal{N}_N(T) = 2\sum_{n=1}^{\lceil N/2\rceil-1}\binom{N}{n},$$
5. *at temperature* $T = N^{-1}$,
$$\mathcal{N}_N(T) = \sum_{n=1}^{\lceil N/2\rceil-1}\binom{N}{n},$$
6. *for temperatures* $0 < T < N^{-1}$,
$$\mathcal{N}_N(T) = \sum_{n=1}^{N-1}\binom{N}{n}.$$

Proof: The result follows from the ISM bifurcation scenario outlined above, when realizing that there are $\binom{N}{n}$ $(n-1)$-faces in an $(N-1)$-simplex and that the SONN renormalization step consists of M independent renormalizations on M standard simplexes S_{N-1}.

1. For $T > T_E(N,1)$ there is a unique fixed point $\overline{\mathbf{w}} \in S_{N-1}$ of ISM (7). Note that there is only one fixed point $\{\overline{\mathbf{w}}\}^M$ of the SONN renormalization step (9) corresponding to the M maximum entropy points $\overline{\mathbf{w}}$ of individual ISM renormalizations.

2. When $T = T_E(N, N_1)$, $N_1 = 1, 2, ..., \lceil N/2 \rceil - 1$, $\binom{N}{N_1}$ ISM fixed points are created on $\binom{N}{N_1}$ lines from $\overline{\mathbf{w}}$ to $(N_1 - 1)$-faces of S_{N-1}. For each $1 \leq n < N_1$, there already exists a pair of ISM fixed points on each of $\binom{N}{n}$ lines from $\overline{\mathbf{w}}$ to $(n-1)$-faces of S_{N-1}. The maximum entropy fixed point $\overline{\mathbf{w}}$ of ISM (7) always exists.

   Because the SONN renormalization step consists of M independent ISM renormalizations on M standard simplexes S_{N-1}, the $1+\mathcal{N}_N(T) = 1 + \binom{N}{N_1} + 2\sum_{n=1}^{N_1-1}\binom{N}{n}$ ISM fixed points translate to $(1 + \mathcal{N}_N(T))^M$ fixed points of the SONN renormalization.

3. For $T_E(N, N_1) < T < T_E(N, N_1 - 1)$, $N_1 = 2, ..., \lceil N/2 \rceil - 1$, for each $1 \leq n < N_1$, there exists a pair of ISM fixed points on each of $\binom{N}{n}$ lines from $\overline{\mathbf{w}}$ to $(n-1)$-faces of S_{N-1}.

4. For $N^{-1} < T < T_E(N, \lceil N/2 \rceil - 1)$, all "paired" ISM fixed points exist, and so for each $1 \leq n < \lceil N/2 \rceil$, there is a pair of ISM fixed points on each of $\binom{N}{n}$ lines from $\overline{\mathbf{w}}$ to $(n-1)$-faces of S_{N-1}.

5. At $T = N^{-1}$, for every $1 \leq n < \lceil N/2 \rceil$, the ISM fixed points closer to $\overline{\mathbf{w}}$ on each of $\binom{N}{n}$ lines from $\overline{\mathbf{w}}$ to $(n-1)$-faces of S_{N-1} seize to exist and those lines now contain a single ISM fixed point each.

6. For $0 < T < N^{-1}$, a single ISM fixed point on each of the lines connecting $\overline{\mathbf{w}}$ with each face[3] of S_{N-1} exists.

Q.E.D.

Having characterized the number and position of equilibria of SONN renormalization, in the next section we present their stability analysis.

5 Stability analysis of renormalization equilibria

The maximum entropy point $\overline{\mathbf{w}}$ is not only a fixed point of ISM (7), but also, regarded as a vector $\overline{\mathbf{w}} - \mathbf{0}_N$, it is an eigenvector of the Jacobian $J(\mathbf{w}; T)$ (see eq. (6)) at any $\mathbf{w} \in S^0_{N-1}$, with eigenvalue $\lambda = 0$ (Kwok and Smith, 2005). This simply reflects the fact that ISM renormalization acts on the standard simplex S_{N-1}, which is a subset of a $(N-1)$-dimensional hyperplane with normal vector $\mathbf{1}_N$.

[3] except for S_{N-1} itself

We have already seen that the maximum entropy point $\overline{\mathbf{w}}$ plays a special role in the ISM equilibria structure: all equilibria lie on lines going from $\overline{\mathbf{w}}$ towards maximum entropy points of faces of S_{N-1}. The lines themselves are of special interest, since we will show that these lines are invariant manifolds of the ISM renormalization and their directional vectors are eigenvectors of ISM Jacobians at the fixed points located on them.

First, we need an auxiliary lemma.

Lemma 5.1 *Let* $\mathbf{w} \in \mathcal{E}_{N,N_1}(\gamma_1)$ *for some* $1 \leq N_1 < N$, $\gamma_1 \in (N^{-1}, N_1^{-1})$, *be a fixed point of ISM (7) with squared Euclidean norm* $\|\mathbf{w}\|^2 = \mathbf{w}'\mathbf{w}$. *Then,* $\gamma_1 > \|\mathbf{w}\|^2$ *and* $\gamma_2 < \|\mathbf{w}\|^2$, *where* $\gamma_2 = (1 - N_1\gamma_1)/(N - N_1)$.

Proof: We have

$$\|\mathbf{w}\|^2 = N_1\gamma_1^2 + N_2\gamma_2^2 = \frac{NN_1\gamma_1^2 - 2N_1\gamma_1 + 1}{N - N_1}.$$

Now, $\|\mathbf{w}\|^2 - \gamma_1 < 0$ only if

$$\kappa(\gamma_1) = NN_1\gamma_1^2 - \gamma_1(N + N_1) + 1 < 0. \tag{25}$$

Given N, N_1, $\kappa(\gamma_1)$ can be considered quadratic function of γ_1 on $\mathbb{R}$ with zeros at $\gamma_1 = N^{-1}$ and $\gamma_1 = N_1^{-1}$. Hence $\kappa(\gamma_1) < 0$ for all γ_1 in (N^{-1}, N_1^{-1}), exactly the allowed range for γ_1.

The statement $\gamma_2 < \|\mathbf{w}\|^2$ can be proved in a completely symmetric manner. *Q.E.D.*

Theorem 5.2 *Let* $\mathbf{w} \in \mathcal{E}_{N,N_1}(\gamma_1)$ *for some* $1 \leq N_1 < N$, $\gamma_1 \in (N^{-1}, N_1^{-1})$, *be a fixed point of ISM (7). Then,* $\mathbf{w}_* = \overline{\mathbf{w}} - \mathbf{w}$ *is an eigenvector of the Jacobian* $J(\mathbf{w}; T_{N,N_1}(\gamma_1))$ *of ISM at* $\mathbf{w}$ *with the corresponding eigenvalue*

$$\lambda_* = \frac{\gamma_1 \cdot (\gamma_1 - \|\mathbf{w}\|^2)}{T_{N,N_1}(\gamma_1) \cdot (\gamma_1 - N^{-1})} > 0, \tag{26}$$

where $\|\mathbf{w}\|^2 = \mathbf{w}'\mathbf{w}$ *is the squared Euclidean norm of* $\mathbf{w}$.

Proof: To simplify the notation, we will denote the Jacobian of ISM at $\mathbf{w} = (w_1, w_2, ..., w_N)'$ by J and the temperature at which $\mathbf{w}$ exists by T. From

$$J\mathbf{w}_* = J(\overline{\mathbf{w}} - \mathbf{w}) = J\overline{\mathbf{w}} - J\mathbf{w} = -J\mathbf{w},$$

and using (6), we have that the i-th element of $J\mathbf{w}_*$ is equal to

$$\frac{w_i}{T}(\mathbf{w}'\mathbf{w} - w_i\mathbf{e}_i'\mathbf{w}) = \frac{w_i}{T}(\|\mathbf{w}\|^2 - w_i).$$

For $\mathbf{w}_*$ to be an eigenvector of J with eigenvalue λ_*, it must hold

$$J\mathbf{w}_* = \lambda_*\overline{\mathbf{w}} - \lambda_*\mathbf{w},$$

and so the i-th element of $J\mathbf{w}_*$ must also be equal to $\lambda_* N^{-1} - \lambda_* w_i$. Hence,

$$\frac{w_i}{T}(\|\mathbf{w}\|^2 - w_i) = \lambda_* N^{-1} - \lambda_* w_i \tag{27}$$

should hold for all $i = 1, 2, ..., N$. But we know that $w_i \in \{\gamma_1, \gamma_2\}$, $\gamma_2 = (1 - N_1\gamma_1)/(N - N_1)$, and so

$$\frac{\gamma_1 \cdot (\gamma_1 - \|\mathbf{w}\|^2)}{\gamma_2 \cdot (\gamma_2 - \|\mathbf{w}\|^2)} = \frac{\gamma_1 - N^{-1}}{\gamma_2 - N^{-1}} \tag{28}$$

would need to be true. Since $\gamma_1, \gamma_2 > 0$, (28) can be rewritten as

$$\frac{\gamma_1 - \|\mathbf{w}\|^2}{\gamma_2 - \|\mathbf{w}\|^2} = \frac{1 - (N\gamma_1)^{-1}}{(1 - N\gamma_2)^{-1}}. \tag{29}$$

To verify whether (29) holds, we write

$$\begin{aligned} \frac{\gamma_1 - \|\mathbf{w}\|^2}{\gamma_2 - \|\mathbf{w}\|^2} &= \frac{\gamma_1 - \|\mathbf{w}\|^2}{\frac{1-N_1\gamma_1}{N-N_1} - \|\mathbf{w}\|^2} \\ &= 1 - \frac{1 - N\gamma_1}{1 - N_1\gamma_1 - (N - N_1)\|\mathbf{w}\|^2}. \end{aligned} \tag{30}$$

and

$$\begin{aligned} \frac{1 - \frac{1}{N\gamma_1}}{1 - \frac{1}{N\gamma_2}} &= \frac{\frac{N\gamma_1 - 1}{N\gamma_1}}{\frac{N_1(N\gamma_1 - 1)}{N(N_1\gamma_1 - 1)}} \\ &= 1 - \frac{1}{N_1\gamma_1}. \end{aligned} \tag{31}$$

We need to show that

$$\frac{1 - N\gamma_1}{1 - N_1\gamma_1 - (N - N_1)\|\mathbf{w}\|^2} = \frac{1}{N_1\gamma_1}. \tag{32}$$

Note that the denominators in (32) are guaranteed to be nonzero, since $N_1, \gamma_1 > 0$ and by lemma 5.1,

$$1 - N_1\gamma_1 - (N - N_1)\|\mathbf{w}\|^2 = 1 - N_1\gamma_1 - N_2\|\mathbf{w}\|^2 < 1 - N_1\gamma_1 - N_2\gamma_2 = 0.$$

Hence, (32) can be restated as

$$N_1\gamma_1(1 - N\gamma_1) = 1 - N_1\gamma_1 - (N - N_1)\|\mathbf{w}\|^2. \tag{33}$$

But (33) holds, since

$$\|\mathbf{w}\|^2 = N_1\gamma_1^2 + N_2\gamma_2^2 = N_1\gamma_1^2 + \frac{(1 - N_1\gamma_1)^2}{N - N_1}. \tag{34}$$

The expression (26) for λ_* follows from (27), by plugging in[4] γ_1 for w_i.

It remains to be shown that λ_* is positive. This follows directly from (26) since $\gamma_1 > N^{-1} > 0$, $T > 0$, and by lemma 5.1, $\gamma_1 - \|\mathbf{w}\|^2 > 0$.

Q.E.D.

Theorem 5.3 *Let* $\mathbf{w} \in \mathcal{E}_{N,N_1}(\gamma_1)$ *for some* $\lceil N/2 \rceil \leq N_1 \leq N - 1$, $\gamma_1 \in (N^{-1}, N_1^{-1})$, *be a fixed point of ISM (7) and* λ_* *be the eigenvalue associated with eigenvector* $\mathbf{w}_* = \overline{\mathbf{w}} - \mathbf{w}$ *of the Jacobian* $J(\mathbf{w}; T_{N,N_1}(\gamma_1))$ *of ISM at* $\mathbf{w}$. *Then,* $0 < \lambda_* < 1$.

Proof:

Using parametrization (20-21),

$$\begin{aligned} \|\mathbf{w}\|^2 &= N_1\gamma_1^2 + N_2\gamma_2^2 \\ &= \frac{1}{N}\left(1 + \tau^2\frac{N_2}{N_1}\right), \end{aligned} \tag{35}$$

so that

$$\begin{aligned} \gamma_1 - \|\mathbf{w}\|^2 &= \frac{1}{N}\left(\tau\frac{N_2}{N_1} - \tau^2\frac{N_2}{N_1}\right) \\ &= \frac{N_2}{N_1 N}\tau(1 - \tau), \end{aligned} \tag{36}$$

[4] alternatively, we could have used γ_2

and since

$$\gamma_1 - N^{-1} = \frac{N_2}{N_1 N}\tau,$$

we can write

$$\frac{\gamma_1 - \|\mathbf{w}\|^2}{\gamma_1 - N^{-1}} = 1 - \tau. \tag{37}$$

From (26) and (37) we obtain

$$\lambda_* = \frac{\gamma_1}{T}(1-\tau). \tag{38}$$

Now, assume $\lambda_* \geq 1$. That means (using (38) and (21))

$$\frac{T}{\gamma_1} = \frac{1 - \frac{\gamma_2}{\gamma_1}}{-\ln \frac{\gamma_2}{\gamma_1}} \leq 1 - \tau = \gamma_1 N \frac{\gamma_2}{\gamma_1},$$

which can be written as

$$\frac{a-1}{\ln a} \leq N\gamma_1 a, \tag{39}$$

where

$$0 < a = \frac{\gamma_2}{\gamma_1} < 1. \tag{40}$$

Since

$$N_1\gamma_1 + (N - N_1)\gamma_2 = N_1\gamma_1 + (N - N_1)a\gamma_1 = 1,$$

we have

$$\gamma_1 = (N_1 + (N - N_1)a)^{-1},$$

and (39) reads[5]

$$\begin{aligned} \ln a &\leq -\frac{1-a}{a}\left(\rho + a(1-\rho)\right) \\ &= -\rho\frac{(1-a)^2}{a} + a - 1 = f(a;\rho). \end{aligned} \tag{41}$$

where

$$0 < \rho = \frac{N_1}{N} < 1. \tag{42}$$

The function $f(a;\rho)$ is increasing on $a \in (0,1)$ (actually on $a > 0$), since its derivative $f'(a) = \rho/a^2 + 1 - \rho$ is positive. The second derivative of f, $f''(a) = -2\rho/a^3$, is negative for $a > 0$, and so $f(a)$ is concave.

[5] $\ln a < 0$

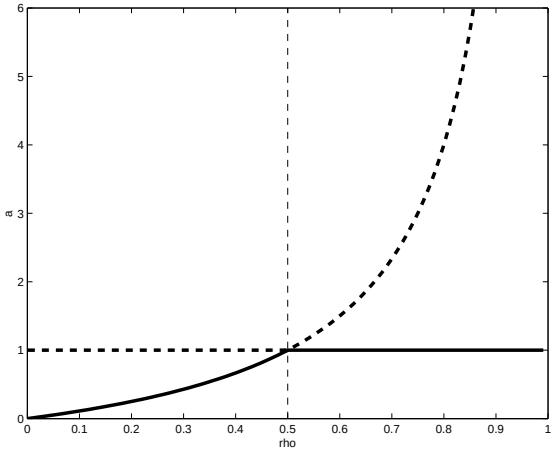

Figure 3: Boundary points a_1 (solid bold line) and a_2 (dashed bold line), plotted as functions of $\rho \in (0,1)$. The quadratic function $g(a)$ (see (43)) is positive for $a < a_1$ and $a > a_2$.

On $a > 0$, both $\ln a$ and $f(a)$ are continuous concave functions with $\ln 1 = f(1) = 0$ and $\ln'(1) = f'(1) = 1$. So the function values, as well as the slopes of $\ln a$ and $f(a)$ coincide at $a = 1$. We will investigate conditions under which the slope of $f(a)$ exceeds that of $\ln a$ on the whole interval $(0,1)$. Then, for $a \in (0,1)$, we would have $f(a) < \ln a$.

The inequality

$$f'(a) - \ln'(a) > 0$$

holds, whenever $1 - \rho + \rho a^{-2} - a^{-1} > 0$, which is equivalent to

$$g(a) = a^2(1-\rho) - a + \rho > 0. \tag{43}$$

Since $1 - \rho > 0$, $g(a) > 0$ on $a \in (0, a_1) \cup (a_2, 1)$, where a_1, a_2 are zeros of the quadratic function $g(a)$,

$$a_{1,2} = \frac{1 \pm |1 - 2\rho|}{2(1-\rho)}. \tag{44}$$

For $\rho \in (0, 1/2)$, we have $a_1 = \rho/(1-\rho)$ and $a_2 = 1$, whereas for $\rho \in [1/2, 1)$, $a_1 = 1$ and $a_2 = \rho/(1-\rho)$. The boundary points a_1 and a_2, plotted as functions of $\rho \in (0,1)$, are shown in figure 3.

Because $N_1 \geq \lceil N/2 \rceil$, we have $\rho \geq 1/2$, and so $g(a) > 0$ on $a \in (0,1)$. But $a = \gamma_2/\gamma_1$ is always in the interval $(0,1)$ (see eq. (40)). It follows that

$f(a) < \ln a$ for any $a \in (0,1)$. This is a contradiction to (41), and so it must be that $\lambda_* < 1$. By theorem 5.2, λ_* is positive. *Q.E.D.*

Theorem 5.4 *Let* $\mathbf{w} \in \mathcal{E}_{N,N_1}(\gamma_1)$ *for some* $1 \leq N_1 < \lceil N/2 \rceil$ *and* $N^{-1} < \gamma_1 < (2N_1)^{-1}$, *be a fixed point of ISM (7) and* λ_* *be the eigenvalue associated with eigenvector* $\mathbf{w}_* = \overline{\mathbf{w}} - \mathbf{w}$ *of the Jacobian* $J(\mathbf{w}; T_{N,N_1}(\gamma_1))$ *of ISM at* $\mathbf{w}$. *Then,* $\lambda_* > 1$.

Proof: First note that the bound $N^{-1} < \gamma_1 < (2N_1)^{-1}$ is well defined, since from $N_1 < N/2$ we have $1/(2N_1) > 1/N$.

The proof proceeds analogously to the proof of theorem 5.3, but this time we are interested in the negative range of $g(a)$, implying $f'(a) < \ln'(a)$. For $a \in (0,1)$, $g(a) < 0$ only on $a \in (a_1, 1)$. Since $\ln a$ and $f(a)$ are continuous concave functions with $\ln 1 = f(1) = 0$, $\ln'(1) = f'(1) = 1$, and $f'(a) < \ln'(a)$, it must be that on $a \in (a_1, 1)$, $f(a) > \ln a$. That means $\lambda_* > 1$.

For $\rho \in (0, 1/2)$,

$$a_1 = \frac{\rho}{1-\rho} = \frac{\frac{N_1}{N}}{\frac{N-N_1}{N}} = \frac{N_1}{N_2}.$$

Now,

$$\frac{1 - N_1\gamma_1}{N_2\gamma_1} = \frac{\gamma_2}{\gamma_1} = a > a_1 = \frac{N_1}{N_2},$$

only if $\gamma_1 < 1/(2N_1)$.

Q.E.D.

Theorem 5.5 *Consider ISM (7) and* $1 \leq N_1 < \lceil N/2 \rceil$. *Then there exists* $\bar{\gamma}_1 \in ((2N_1)^{-1}, N_1^{-1})$, *such that for all ISM fixed points* $\mathbf{w} \in \mathcal{E}_{N,N_1}(\gamma_1)$ *with* $\gamma_1 \in (\bar{\gamma}_1, N_1^{-1})$, *the eigenvalue associated with eigenvector* $\mathbf{w}_* = \overline{\mathbf{w}} - \mathbf{w}$ *of the Jacobian* $J(\mathbf{w}; T_{N,N_1}(\gamma_1))$ *of ISM at* $\mathbf{w}$ *is positive and less than 1, e.g.* $0 < \lambda_* < 1$.

Proof: Based on proof of theorem 5.3, for $a \in (0, a_1)$, we have $f'(a) > \ln'(a)$. This corresponds to $\gamma_1 > 1/(2N_1)$ (see proof of theorem 5.4).

Now, $\ln a$ and $f(a)$ are continuous concave functions with $\ln 1 = f(1) = 0$, $\ln'(1) = f'(1) = 1$, and on $a \in (a_1, 1)$, we have $f'(a) < \ln'(a)$, implying that for $a \in (a_1, 1)$, $\ln a < f(a)$.

Since

$$\lim_{a\to 0^+} f(a) = \lim_{a\to 0^+} \ln a = \infty$$

and (using L'Hospital rule)

$$\lim_{a\to 0^+} \frac{\ln a}{f(a)} = 0,$$

there exists $\bar{a} \in (0, a_1)$, such that on $a \in (0, \bar{a})$, $f(a) < \ln a$ (both $f(a)$ and $\ln a$ are negative). The coordinate $\bar{\gamma}_1$ corresponds to the value $\bar{a}$. Since $\bar{a} < a_1$, we have $\bar{\gamma}_1 > 1/(2N_1)$. Furthermore, $a \in (0, \bar{a})$ corresponds to $\gamma_1 \in (\bar{\gamma}_1, N_1^{-1})$.

Q.E.D.

Theorem 5.6 *Consider ISM (7) and $1 \le N_1 < N$. Then for each maximum entropy point $\widetilde{\mathbf{w}} \in \mathcal{Q}_{N,N_1}$ of an $(N_1 - 1)$-face of S_{N-1}, the line $\ell(\tau; \overline{\mathbf{w}}, \widetilde{\mathbf{w}})$, $t \in [0, 1)$ (eqs. (20-21)), connecting the maximum entropy point $\overline{\mathbf{w}}$ with $\widetilde{\mathbf{w}}$ is an invariant set under the ISM dynamics.*

Proof: Without loss of generality, consider the canonical form of $\widetilde{\mathbf{w}} \in \mathcal{Q}_{N,N_1}$, namely

$$\widetilde{\mathbf{w}} = \overline{\mathbf{w}}_{N,N_1} = \frac{1}{N_1}(\mathbf{1}'_{N_1}, \mathbf{0}'_{N-N_1})',$$

a parameter value $\tau \in [0, 1)$ and the point $\mathbf{w}(\tau) = \ell(\tau; \overline{\mathbf{w}}, \widetilde{\mathbf{w}})$ addressed by it on the line connecting $\overline{\mathbf{w}}$ with $\widetilde{\mathbf{w}} \in \mathcal{Q}_{N,N_1}$. The image $\mathbf{F}(\mathbf{w}(\tau))$ of $\mathbf{w}(\tau)$ under the ISM has the following form:

$$\begin{aligned} \gamma_1 = F_i(\mathbf{w}(\tau)) &= \frac{\exp\{\frac{1}{TN}(1-\tau) + \frac{1}{TN_1}\tau\}}{N_1 \exp\{\frac{1}{TN}(1-\tau) + \frac{1}{TN_1}\tau\} + N_2 \exp\{\frac{1}{TN}(1-\tau)\}} \\ &= \frac{\exp\{\frac{1}{TN_1}\tau\}}{N_1 \exp\{\frac{1}{TN_1}\tau\} + N_2}, \quad i = 1, 2, ..., N_1, \end{aligned} \tag{45}$$

and

$$\gamma_2 = F_i(\mathbf{w}(\tau)) = \frac{\exp\{\frac{1}{TN}(1-\tau)\}}{N_1 \exp\{\frac{1}{TN}(1-\tau) + \frac{1}{TN_1}\tau\} + N_2 \exp\{\frac{1}{TN}(1-\tau)\}}$$

$$= \frac{1}{N_1 \exp\{\frac{1}{TN_1}\tau\} + N_2}, \quad i = N_1+1, N_1+2, ..., N. \quad (46)$$

Denoting $N_1 \exp\{\frac{1}{TN_1}\tau\} + N_2$ by Z, the parameter value τ giving $\gamma_2 = Z^{-1}$ under the line parametrization (21) is

$$\tau^* = 1 - \frac{N}{Z}. \quad (47)$$

Plugging τ^* into the parametrization (20) for γ_1 yields

$$\frac{Z + N_1 - N}{ZN_1} = \frac{Z - N_2}{ZN_1} = \frac{\exp\{\frac{1}{TN_1}\tau\}}{Z}.$$

So the image under ISM map $\mathbf{F}$ of any point $\mathbf{w}(\tau) = \ell(\tau; \overline{\mathbf{w}}, \widetilde{\mathbf{w}})$, $\tau \in [0.1)$, can be written as $\mathbf{F}(\mathbf{w}(\tau)) = \ell(\tau^*; \overline{\mathbf{w}}, \widetilde{\mathbf{w}})$, where $0 \leq \tau^* = 1 - N/Z < 1$.

Q.E.D.

We have established that for any fixed point $\mathbf{w} \in S^0_{N-1}$ of ISM (7), $\mathbf{w}_* = \overline{\mathbf{w}} - \mathbf{w}$ is always an eigendirection of the linearized system at $\mathbf{w}$. If $\mathbf{w} \in \mathcal{E}_{N,N_1}(\gamma_1)$ for some $\lceil N/2 \rceil \leq N_1 < N$, $\gamma_1 \in (N^{-1}, N_1^{-1})$, the eigendirection $\mathbf{w}_*$ is stable with non-oscillatory behavior, i.e. the associated eigenvalue λ_* of the ISM Jacobian at $\mathbf{w}$ is a real positive number, smaller than 1. If $1 \leq N_1 < \lceil N/2 \rceil$, the eigendirection $\mathbf{w}_*$ is stable for fixed points close enough to the maximum entropy points of faces of S_{N-1}, for those close to $\overline{\mathbf{w}}$, the eigendirection $\mathbf{w}_*$ is unstable. Moreover, $\mathbf{1}_N$ is always an eigendirection of the linearized ISM system with zero eigenvalue. As mentioned earlier, this is due to the fact that ISM renormalization acts on the standard simplex S_{N-1}, which is part of an $(N-1)$-dimensional hyperplane with normal vector $\mathbf{1}_N$.

We now continue with analysis of the remaining $N-2$ eigendirections of the linearized ISM system at its fixed points $\mathbf{w}$. Recall that $\Gamma(\mathbf{w}) \in \mathcal{Q}_{N,N_1}$ denotes the maximum entropy point of an (N_1-1)-face of S_{N-1}, such that $\mathbf{w}$ lies on the line segment connecting $\overline{\mathbf{w}}$ with $\Gamma(\mathbf{w})$.

Theorem 5.7 *Consider a ISM fixed point $\mathbf{w} \in \mathcal{E}_{N,N_1}(\gamma_1)$ for some $1 \leq N_1 < N$ and $N^{-1} < \gamma_1 < N_1^{-1}$. Let π be a permutation of $\overline{\mathbf{w}}_{N,N_1} = \frac{1}{N_1}(\mathbf{1}'_{N_1}, \mathbf{0}'_{N-N_1})'$ such that $\pi(\overline{\mathbf{w}}_{N,N_1}) = \Gamma(\mathbf{w})$. Let $\mathcal{B} = \{\mathbf{u}_1, \mathbf{u}_2, ..., \mathbf{u}_{N-N_1-1}\}$ be a set of $(N-N_1)$-dimensional unit vectors, such that $\mathcal{B}$, together with $\mathbf{1}_{N-N_1}/\|\mathbf{1}_{N-N_1}\|$, form an orthonormal basis of $\mathbb{R}^{N-N_1}$. Then, there are $N-N_1-1$ eigenvectors of the Jacobian $J(\mathbf{w}; T_{N,N_1}(\gamma_1))$ of ISM at $\mathbf{w}$ of the form:*

$$\mathbf{v}^i_- = \pi((\mathbf{0}'_{N_1}, \mathbf{u}'_i)'), \quad i = 1, 2, ..., N-N_1-1. \quad (48)$$

All eigenvectors $\mathbf{v}_-^1, \mathbf{v}_-^2, ..., \mathbf{v}_-^{N-N_1-1}$ *have the same associated eigenvalue*

$$0 < \lambda_- = \frac{1 - N_1\gamma_1}{(N - N_1)T_{N,N_1}(\gamma_1)} < 1. \tag{49}$$

Proof: Without loss of generality assume that $\mathbf{w} = (\gamma_1 \mathbf{1}'_{N_1}, \gamma_2 \mathbf{1}'_{N_2})'$, where γ_2 is defined by (14) and $N_2 = N - N_1$. All the results translate to permutations of $\mathbf{w}$ in a straightforward manner.

To simplify the notation, we will denote the Jacobian $J(\mathbf{w}; T_{N,N_1}(\gamma_1))$ by J and the temperature $T_{N,N_1}(\gamma_1)$ at which $\mathbf{w}$ exists by T. The n-dimensional identity matrix is denoted by I_n.

The Jacobian can be written as

$$J = \frac{-1}{T} \begin{bmatrix} G_1 & G_{12} \\ G'_{12} & G_2 \end{bmatrix}, \tag{50}$$

where G_1 is an $N_1 \times N_1$ symmetric matrix

$$G_1 = \gamma_1(\gamma_1 \mathbf{1}_{N_1}\mathbf{1}'_{N_1} - I_{N_1}), \tag{51}$$

G_2 is an $N_2 \times N_2$ symmetric matrix

$$G_2 = \gamma_2(\gamma_2 \mathbf{1}_{N_2}\mathbf{1}'_{N_2} - I_{N_2}), \tag{52}$$

and G_{12} is an $N_1 \times N_2$ matrix

$$G_{12} = \gamma_1\gamma_2 \mathbf{1}_{N_1}\mathbf{1}'_{N_2}. \tag{53}$$

For $\mathbf{u} = (u_1, u_2, ..., u_{N_2})' \in \mathcal{B}$,

$$\begin{bmatrix} G_{12} \\ G_2 \end{bmatrix} \mathbf{u} = \begin{bmatrix} \gamma_1\gamma_2\Sigma(\mathbf{u})\mathbf{1}_{N_1} \\ \gamma_2^2\Sigma(\mathbf{u})\mathbf{1}_{N_2} - \gamma_2\mathbf{u} \end{bmatrix},$$

where $\Sigma(\mathbf{u}) = \sum_{i=1}^{N_2} u_i$. All $\mathbf{u} \in \mathcal{B}$ are orthogonal to $\mathbf{1}_{N_2}$, implying that $\Sigma(\mathbf{u}) = 0$. Hence,

$$\begin{bmatrix} G_{12} \\ G_2 \end{bmatrix} \mathbf{u} = -\gamma_2 \begin{bmatrix} \mathbf{0}_{N_1} \\ \mathbf{u} \end{bmatrix}.$$

It follows that for all $i = 1, 2, ..., N - N_1 - 1$,

$$J\mathbf{v}_-^i = \frac{\gamma_2}{T}\mathbf{v}_-^i,$$

meaning that $\mathbf{v}^i_-$ is an eigenvector of J with eigenvalue $\lambda_- = \gamma_2/T$. Now, $\lambda_- > 0$, since $\gamma_2 > 0$ and $T > 0$. It remains to be shown that $\lambda_- < 1$.

By (24),

$$\lambda_- = \frac{\ln \frac{\gamma_1}{\gamma_2}}{\frac{\gamma_1}{\gamma_2} - 1} = \frac{\ln b}{b-1}, \tag{54}$$

where $b = \gamma_1/\gamma_2 > 1$. But $0 < \ln b < b - 1$ on $b \in (1, \infty)$ and so $\lambda_- < 1$. *Q.E.D.*

Theorem 5.8 *Consider a ISM fixed point* $\mathbf{w} \in \mathcal{E}_{N,N_1}(\gamma_1)$ *for some* $1 \leq N_1 < N$ *and* $N^{-1} < \gamma_1 < N_1^{-1}$. *Let* π *be a permutation of* $\overline{\mathbf{w}}_{N,N_1} = \frac{1}{N_1}(\mathbf{1}'_{N_1}, \mathbf{0}'_{N-N_1})'$ *such that* $\pi(\overline{\mathbf{w}}_{N,N_1}) = \Gamma(\mathbf{w})$. *Let* $\mathcal{B} = \{\mathbf{u}_1, \mathbf{u}_2, ..., \mathbf{u}_{N_1-1}\}$ *be a set of* N_1*-dimensional unit vectors, such that* $\mathcal{B}$*, together with* $\mathbf{1}_{N_1}/\|\mathbf{1}_{N_1}\|$*, form an orthonormal basis of* $\mathbb{R}^{N_1}$. *Then, there are* $N_1 - 1$ *eigenvectors of the Jacobian* $J(\mathbf{w}; T_{N,N_1}(\gamma_1))$ *of ISM at* $\mathbf{w}$ *of the form:*

$$\mathbf{v}^i_+ = \pi((\mathbf{u}'_i, \mathbf{0}'_{N-N_1})'), \quad i = 1, 2, ..., N_1 - 1. \tag{55}$$

All eigenvectors $\mathbf{v}^1_+, \mathbf{v}^2_+, ..., \mathbf{v}^{N_1-1}_+$ *have the same associated eigenvalue*

$$\lambda_+ = \frac{\gamma_1}{T_{N,N_1}(\gamma_1)} > 1. \tag{56}$$

Proof: Using arguments analogous to those in the proof of theorem 5.7 one obtains that for all $i = 1, 2, ..., N_1 - 1$,

$$J\mathbf{v}^i_+ = \frac{\gamma_1}{T}\mathbf{v}^i_+.$$

By (24),

$$\lambda_+ = \frac{\ln \frac{\gamma_2}{\gamma_1}}{\frac{\gamma_2}{\gamma_1} - 1} = \frac{\ln a}{a-1}, \tag{57}$$

where $0 < a = \gamma_2/\gamma_1 < 1$. By noting that on $a \in (0, 1)$, $\ln a < a - 1 < 0$, we get $\lambda_+ > 1$.

Q.E.D.

5.1 Illustrative example

As a simple illustration of the ISM equilibria organization, we show in figure 4 positions of low temperature ISM equilibria for $N = 3$. The equilibria (filled circles) are located on the lines connecting the maximum entropy point $\overline{\mathbf{w}}$ with maximum entropy points of faces of S_2. Only one fixed point exists on each line. Triangles and squares represent maximum entropy points of 0-faces (vertices) and 1-faces (edges), respectively. For some fixed points $\mathbf{w}$ we also show eigenvectors of the local Jacobian J. Note that the vector $\overline{\mathbf{w}}$, pointing out of simplex S_2, is always an eigenvector of J (with eigenvalue 0). Also, $\mathbf{w}_* = \overline{\mathbf{w}} - \mathbf{w}$, pointing towards the maximum entropy point $\overline{\mathbf{w}}$, is an eigenvector of J. The remaining eigenvector must be orthogonal to both $\overline{\mathbf{w}}$ and $\mathbf{w}_*$. The flow on S_2 related to this ISM configuration is illustrated in figure 5. Unstable maximum entropy equilibrium $\overline{\mathbf{w}}$ is surrounded by saddle points on lines connecting $\overline{\mathbf{w}}$ with maximum entropy points of edges of S_2. The lines themselves form stable manifolds of the saddle points (the eigenvalue λ_* is positive and < 1 and the lines are invariant sets of the ISM dynamics). Flows initiated outside such lines converge towards stable points located on the lines connecting $\overline{\mathbf{w}}$ with vertices of S_2. Note that the stable manifolds of saddle equilibria (lines from $\overline{\mathbf{w}}$ to the maximum entropy points of edges of S_2) are boundaries of basins of attraction of the stable equilibria. Sample trajectories (projected onto the first two coordinates) in such an ISM are shown in figure 6. The unstable equilibrium $\overline{\mathbf{w}}$, saddle and stable equilibria are shown as circle, diamonds and stars, respectively.

5.2 Equilibria near vertices of the standard simplex

We have proved that components of *stable* equilibria of the SONN renormalization can only be found near vertices $\mathbf{w}_0$ of the ISM simplexes S_{N-1}, on the lines $\ell(\tau; \overline{\mathbf{w}}, \mathbf{w}_0)$ connecting the maximum entropy point $\overline{\mathbf{w}}$ with the vertices $\mathbf{w}_0$. This corresponds to the case $N_1 = 1$. Stable manifold of the linearized ISM system at such an equilibrium $\mathbf{w} \in S^0_{N-1}$ is given by the span of $\mathbf{w}_* = \overline{\mathbf{w}} - \mathbf{w}$ (by theorem 5.5 the corresponding eigenvalue λ_* is in $(0, 1)$ if $\mathbf{w}$ lies sufficiently close to the vertex $\mathbf{w}_0 = \Gamma(\mathbf{w})$ of S_{N-1}) and $N - 2$ vectors orthogonal to $\overline{\mathbf{w}}$ and $\mathbf{w}_*$ (theorem 5.7). Since $N_1 = 1$, there is no invariant manifold of the linearized ISM with expansion rate $\lambda_+ > 1$ (theorem 5.8). Also, no dynamics takes place outside interior of S_{N-1} (zero eigenvalue corresponding to the eigenvector $\overline{\mathbf{w}}$ of the linearized ISM). Note that by theorem 5.8, *all* ISM fixed points with $N_1 \geq 2$ are unstable.

By theorem 4.6, ISM equilibria with $N_1 = 1$ can only exist at temper-

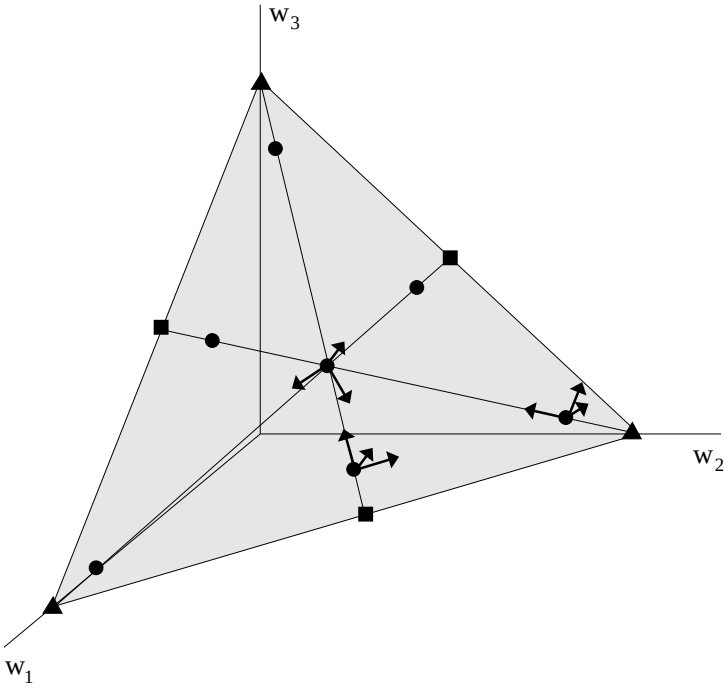

Figure 4: Positions of ISM equilibria (filled circles) for $N = 3$ at a low temperature. The equilibria are located on the lines connecting the maximum entropy point $\overline{\mathbf{w}}$ with maximum entropy points of faces of S_2, namely 0-faces (triangles) and 1-faces (squares). Only one fixed point exists on each line. For some fixed points $\mathbf{w}$ eigenvectors of the local Jacobian J are shown. Vector $\overline{\mathbf{w}}$, pointing out of simplex S_2, is always an eigenvector of J (with eigenvalue 0). Vector $\mathbf{w}_* = \overline{\mathbf{w}} - \mathbf{w}$, pointing towards the maximum entropy point $\overline{\mathbf{w}}$, is an eigenvector of J as well. The remaining eigenvector must be orthogonal to both $\overline{\mathbf{w}}$ and $\mathbf{w}_*$.

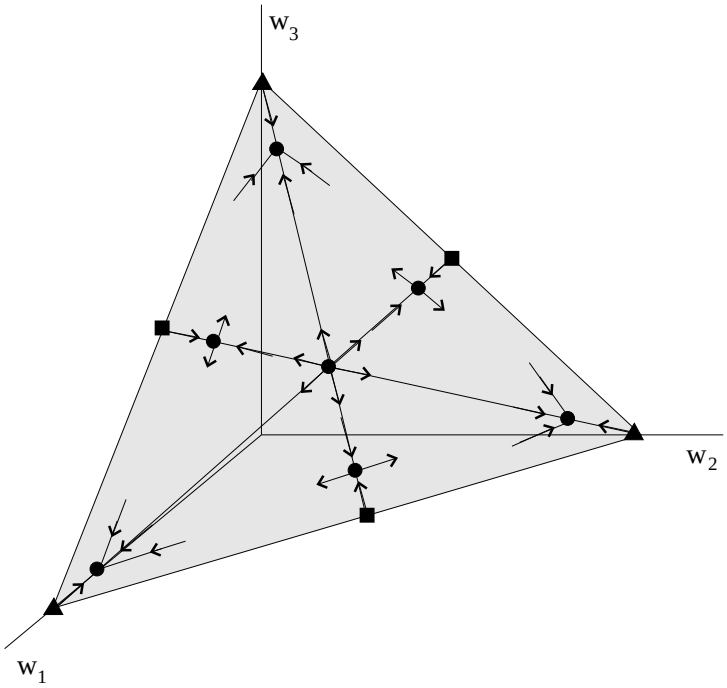

Figure 5: ISM flow on S_2 for $N = 3$ at a low temperature. Unstable maximum entropy equilibrium $\overline{\mathbf{w}}$ is surrounded by saddle points on the lines connecting $\overline{\mathbf{w}}$ with maximum entropy points of edges of S_2. The lines themselves form stable manifolds of the saddle points. Flows initiated outside such lines converge towards stable points located on the lines connecting $\overline{\mathbf{w}}$ with vertices of S_{N-1}. Stable manifolds of saddle equilibria are boundaries of basins of attraction of the stable equilibria.

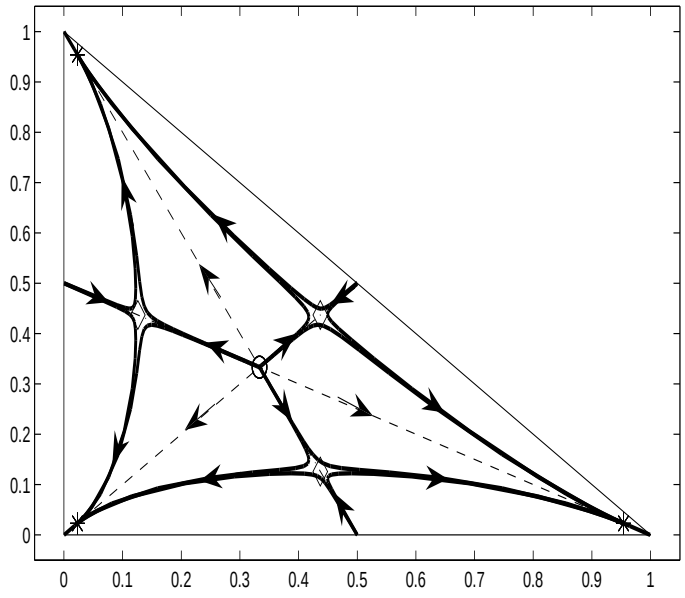

Figure 6: Sample trajectories (projected onto the first two coordinates) in a low temperature ISM for $N = 3$ ($T = 1/4 < 1/N = 1/3$). The unstable equilibrium $\overline{\mathbf{w}}$, saddle and stable equilibria are shown as circle, diamonds and stars, respectively.

atures $T \in (0, T_E(N,1))$. By theorem 4.2, for each vertex $\mathbf{w}_0$ of S_{N-1}, at temperature $T \in (N^{-1}, T_E(N,1))$, there are exactly two equilibria $\mathbf{w}_-(T)$ and $\mathbf{w}_+(T)$ on the line $\ell(\tau; \overline{\mathbf{w}}, \mathbf{w}_0)$. As the temperature decreases, $\mathbf{w}_-(T)$ and $\mathbf{w}_+(T)$ move towards $\overline{\mathbf{w}}$ and $\mathbf{w}_0$, respectively.

In this section we show that $\mathbf{w}_+(T)$ is a stable equilibrium with increasingly strong attraction rate as the system cools down, while $\mathbf{w}_-(T)$ a saddle ISM fixed point.

Let $\mathbf{w} \in \{\mathbf{w}_-(T), \mathbf{w}_+(T)\}$. By theorem 5.2, $\overline{\mathbf{w}} - \mathbf{w}$ is an eigenvector of the ISM Jacobian at $\mathbf{w}$ with the corresponding positive eigenvalue

$$\begin{aligned} \lambda_*(\gamma_1) &= \frac{\gamma_1 \cdot \left(\gamma_1 - \frac{(1-\gamma_1)^2}{N-1} - \gamma_1^2\right)}{T(\gamma_1 - N^{-1})} \\ &= \frac{N\gamma_1(1-\gamma_1)}{N\gamma_1 - 1} \ln \frac{(N-1)\gamma_1}{1-\gamma_1}. \end{aligned} \tag{58}$$

It is straightforward to show that on $\gamma_1 \in (N^{-1}, 1)$, $\lambda_*(\gamma_1)$ is a concave function of positive slope at[6] $\gamma_1 = N^{-1}$ with $\lim_{\gamma_1 \to N^{-1}} \lambda_*(\gamma_1) = 1$ and $\lim_{\gamma_1 \to 1} \lambda_*(\gamma_1) = 0$. Hence there exists a unique $\gamma_1^* \in (N^{-1}, 1)$, such that $\lambda_*(\gamma_1^*) = 1$ and for $\gamma_1 \in (N^{-1}, \gamma_1^*)$ we have $\lambda_*(\gamma_1) > 1$, whereas for $\gamma_1 \in (\gamma_1^*, 1)$ it holds $0 < \lambda_*(\gamma_1) < 1$.

From (58) and $\lambda_*(\gamma_1^*) = 1$, we have

$$\ln \frac{(N-1)\gamma_1^*}{1-\gamma_1^*} = \frac{N\gamma_1^* - 1}{N\gamma_1^*(1-\gamma_1^*)}. \tag{59}$$

We already know that the temperature function $T_{N,1}(\gamma_1)$ (eq. (16)) is concave, attaining maximum at the first bifurcation temperature $T_E(N,1)$. The derivative of $T_{N,1}(\gamma_1)$ reads

$$T'_{N,1}(\gamma_1) = \frac{1}{(N-1)\ln \frac{(N-1)\gamma_1}{1-\gamma_1}} \left[N - \frac{N\gamma_1 - 1}{\gamma_1(1-\gamma_1)\ln \frac{(N-1)\gamma_1}{1-\gamma_1}} \right]. \tag{60}$$

By plugging in (59) into (60) we obtain $T'_{N,1}(\gamma_1^*) = 0$. It follows that $T_{N,1}(\gamma_1^*) = T_E(N,1)$. Hence for $T \in (N^{-1}, T_E(N,1)$, the eigenvalue λ_* is greater and smaller than 1 for $\mathbf{w}_-(T)$ and $\mathbf{w}_+(T)$, respectively. Note that as the system is annealed, the eigenvalue $0 < \lambda_*(\gamma_1) < 1$ corresponding to $\mathbf{w}_+(T)$ is decreasing. At the same time, $\mathbf{w}_+(T)$ approaches the corresponding vertex $\mathbf{w}_0$ of S_{N-1} along the line $\ell(\tau; \overline{\mathbf{w}}, \mathbf{w}_0)$. The contraction rate in

[6] $\lambda_*(\gamma_1)$ can be continuously extended to $\gamma_1 = 1/N$

the vicinity of $\mathbf{w}_+(T)$ along the line $\ell(\tau; \overline{\mathbf{w}}, \mathbf{w}_0)$ (direction of the eigenvector $\overline{\mathbf{w}} - \mathbf{w}_+(T)$) gets stronger and stronger. The weakest contraction is at equilibria $\mathbf{w}_+(T)$ existing at temperatures close to $T_E(N, 1)$.

It can be easily shown that the other contraction rate (theorem 5.7, (49)),

$$\lambda_-(\gamma_1) = \frac{1 - \gamma_1}{(N-1)T_{N,1}(\gamma_1)}, \tag{61}$$

is a decreasing function of γ_1 as well. Hence, $\mathbf{w}_+(T)$ are stable equilibria with weakest contraction for temperatures close to $T_E(N, 1)$. As the system cools down the contraction gets increasingly strong.

6 Discussion

We have explained how the spatial structure of ISM equilibria evolves as the systems cools down. We have also studied stability types of ISM fixed points. It turns out that for an (M, N)-SONN, the stability type of an ISM fixed point $\mathbf{w} \neq \overline{\mathbf{w}}$ is determined solely by the number N_1 of its coordinates taking value $\gamma_1 > 1/N$ and the value γ_1 itself. The line $\ell(\tau; \overline{\mathbf{w}}, \Gamma(\mathbf{w}))$ contains $\mathbf{w}$ and is an invariant set with respect to the ISM dynamics. The behavior of ISM in the neighborhood of $\mathbf{w}$ is given by the structure of stable and unstable manifolds of the linearized system at $\mathbf{w}$ and that again is determined solely by N_1 and γ_1.

In the intermittent search regime by SONN (Kwok and Smith, 2005), the search is driven by pulling promising solutions temporarily to the vicinity of the 0-1 "one-hot" assignment values (vertices of S_{N-1}) (Tiňo, 2007). The critical temperature for intermittent search should correspond to the case where the attractive forces already exist in the form of attractive equilibria near the "one-hot" assignment suggestions (vertices of S_{N-1}), but the convergence rates towards such equilibria should be sufficiently weak so that the intermittent character of the search is not destroyed. We proved in section 5.2 that this happens for temperatures close to the first bifurcation temperature $T_E(N, 1)$ (defined in theorem 4.2).

In (Kwok and Smith, 2005) it is hypothesised that there is a strong link between the critical temperature for intermittent search by SONN and bifurcation temperatures of the autonomous ISM. In (Tiňo, 2007) we hypothesised (in accordance with (Kwok and Smith, 2005)) that even though there are many potential ISM equilibria, the critical bifurcation points are related only to equilibria near the vertices of S_{N-1}, as only those could be *guaranteed* by the theory of (Tiňo, 2007) (stability bounds) to be stable,

even though the theory did not prevent the other equilibria from being stable. In this study, we have proved that the stable equilibria can in fact exist only near the vertices of S_{N-1}, on the lines connecting $\overline{\mathbf{w}}$ with the vertices. So the critical temperature must be smaller than, but close to $T_E(N,1)$.

As the SONN system cools down, by theorems 4.1 - 4.6, more and more ISM equilibria emerge on the lines connecting the maximum entropy point $\overline{\mathbf{w}}$ of the standard simplex S_{N-1} with the maximum entropy points of its faces of increasing dimensionality. One or two fixed points can exist on the lines connecting $\overline{\mathbf{w}}$ with maximum entropy points of (N_1-1)-faces of S_{N-1}, where $N_1 < N/2$. There can be only one fixed point on each of the lines connecting $\overline{\mathbf{w}}$ with maximum entropy points of higher dimensional faces of S_{N-1}, in particular (N_1-1)-faces of S_{N-1} with $N_1 \geq N/2$.

With decreasing temperature, the dimensionality of stable and unstable manifolds of linearized ISM at emerging equilibria decreases and increases, respectively. At lower temperatures, this creates a peculiar pattern of saddle type equilibria surrounding the unstable maximum entropy point $\overline{\mathbf{w}}$, with decision enforcing "one-hot" stable equilibria located near vertices of S_{N-1}. Trajectory towards the solution as the SONN system anneals is shaped by the complex skeleton of saddle type equilibria with stable/unstable manifolds of varying dimensionalities and can therefore, in synergy with the input driving process, exhibit signatures of a very complex dynamical behavior, as reported e.g. in (Kwok and Smith, 2004). Of course, as explained in section 5.2, once the temperature is sufficiently low, the attraction rates of stable equilibria near the vertices of S_{N-1} are so high that the found solution is virtually pinned down by the system.

We stress that the theory developed in this paper can be applied to other assignment optimization systems that incorporate the softmax assignment weight renormalization (e.g. (Gold and Rangarajan, 1996; Rangarajan, 2000)).

Even though the present study clarifies the prominent role of the first (symmetry breaking) bifurcation temperature $T_E(N,1)$ in obtaining the SONN intermittent search regime and helps to understand the origins of complex SONN adaptation patterns in the annealing regime, many interesting open questions remain. For example, no theory as yet exists for the full SONN adaptation dynamics (Hebbian + renormalization steps). Also, it is not clear exactly how the notion of abstract neighborhood of the winner node supports the existence of intermittent search in SONN. Kwok and Smith (2005) and Tiňo (2007) report a rather strong pattern of increasing neighborhood size with increasing assignment problem size (tested on N-queens), but this issue deserves a more detailed study.

7 Conclusion

Self-organizing neural networks (SONN) driven by softmax weight renormalization (Kwok and Smith, 2000) are capable of finding high quality solutions of difficult assignment optimization problems. Even though the introduction of softmax weight renormalization with temperature parameter can greatly enhance the quality of obtained solutions, the system can be sensitive to annealing schedules and can exhibit complex adaptation patterns as the system cools down. Moreover, it has been recently discovered that there exists a critical temperature setting T_* at which SONN is capable of powerful intermittent search through a multitude of high quality solutions represented as meta-stable states of the SONN dynamics (Kwok and Smith, 2005).

Following (Kwok and Smith, 2005; Tiňo, 2007), we studied SONN adaptation dynamics by concentrating on the autonomous renormalization process that drives the search dynamics in SONN. We performed a detailed bifurcation study of the renormalization process and for each emerging equilibrium gave exact characterization of stable/unstable manifolds of the linearized dynamics.

As the (M, N)-SONN system cools down, new ISM equilibria emerge on the lines connecting the maximum entropy point $\overline{\mathbf{w}}$ of the standard simplex S_{N-1} with the maximum entropy points of its faces of increasing dimensionality. Depending on the face dimensionality, one or two fixed points can exist on each line. The dimensionality of stable and unstable manifolds of linearized ISM at emerging equilibria decreases and increases, respectively as the temperature decreases. At low temperatures, a complex skeleton of saddle type equilibria surrounding the unstable maximum entropy point $\overline{\mathbf{w}}$, with decision enforcing "one-hot" stable equilibria located near vertices of S_{N-1} gradually emerges. This, in synergy with the input driving process, can lead to adaptation processes exhibiting signatures of complex dynamical behavior and sensitivity to annealing schedules.

We have also rigorously shown that (as hypothesized by Kwok and Smith (2005)) the intermittent search by SONN can occur only at temperatures close to the first (symmetry breaking) bifurcation temperature $T_E(N, 1)$, as only then can weakly attractive equilibria of the renormalization process exist. In fact, the only stable equilibria can be found on the lines connecting $\overline{\mathbf{w}}$ with vertices of the standard simplex S_{N-1}. Weakly attractive fixed points close to such vertices shape meta-stable states of the intermittent search dynamics.

Finally, softmax renormalization has been used in other optimization frameworks e.g. in (Gold and Rangarajan, 1996; Rangarajan, 2000), and

the theory developed in this paper can be used for analyzing those settings as well.

References

S. Gold and A. Rangarajan. Softmax to softassign: Neural network algorithms for combinatorial optimization. *Journal of Artificial Neural Networks*, 2(4):381–399, 1996.

F. Guerrero, S. Lozano, K.A. Smith, D. Canca, and T. Kwok. Manufacturing cell formation using a new self-organizing neural network. *Computers & Industrial Engineering*, 42:377–382, 2002.

T. Kohonen. The self-organizing map. *Proceedings of the IEEE*, 78(9): 1464–1479, 1990.

T. Kwok and K.A. Smith. Improving the optimisation properties of a self-organising neural network with weight normalisation. In *Proceedings of the ICSC Symposia on Intelligent Systems and Applications (ISA 2000)*, Paper No.1513-285, 2000.

T. Kwok and K.A. Smith. Performance-enhancing bifurcations in a self-organising neural network. In *Computational Methods in Neural Modeling: Proceedings of the 7th International Work-Conference on Artificial and Natural Neural Networks (IWANN'2003)*, volume Lecture Notes in Computer Science, vol. 2686, pages 390–397, Singapore, 2003. Springer-Verlag, Berlin.

T. Kwok and K.A. Smith. A noisy self-organizing neural network with bifurcation dynamics for combinatorial optimization. *IEEE Transactions on Neural Networks*, 15(1):84–88, 2004.

T. Kwok and K.A. Smith. Optimization via intermittency with a self-organizing neural network. *Neural Computation*, 17:2454–2481, 2005.

A. Rangarajan. Self-annealing and self-annihilation: unifying deterministic annealing and relaxation labeling. *Pattern Recognition*, 33(4):635–649, 2000.

K.A. Smith. Solving the generalized quadratic assignment problem using a self-organizing process. In *Proceedings of the IEEE Int. Conf. on Neural Networks*, volume 4, pages 1876–1879, 1995.

K.A. Smith. Neural networks for combinatorial optimization: a review of more than a decade of research. *INFORMS Journal on Computing*, 11 (1):15–34, 1999.

K.A. Smith, M. Palaniswami, and M. Krishnamoorthy. Neural techniques for combinatorial optimization with applications. *IEEE Transactions on Neural Networks*, 9(6):1301–1318, 1998.

P. Tiňo. Equilibria of iterative softmax and critical temperatures for intermittent search in self-organizing neural networks. *Neural Computation*, 19(4):1056–1081, 2007.